HHS Public Access

Author manuscript

Brain Imaging Behav. Author manuscript; available in PMC 2019 October 01.

Published in final edited form as:

Brain Imaging Behav. 2018 October ; 12(5): 1271–1278. doi:10.1007/s11682-017-9783-y.

Basal ganglia cerebral blood flow associates with psychomotor speed in adults with type 1 diabetes

John P. Ryan[1], **Howard J. Aizenstein**[1], **Trevor J. Orchard**[2], **Karen A. Nunley**[3], **Helmet Karim**[4], and **Caterina Rosano**[3]

[1]Department of Psychiatry, University of Pittsburgh School of Medicine, 3811 O'Hara St., Pittsburgh, PA 15213, USA

[2]Department of Epidemiology, Diabetes and Lipid Research Building, University of Pittsburgh Graduate School of Public Health, Pittsburgh, PA, USA

[3]Department of Epidemiology, University of Pittsburgh Graduate School of Public Health, Pittsburgh, PA, USA

[4]Department of Bioengineering, University of Pittsburgh Swanson School of Engineering, Pittsburgh, PA, USA

Abstract

Type 1 diabetes is associated with slower psychomotor speed, but the neural basis of this relationship is not yet understood. The basal ganglia are a set of structures that are vulnerable to small vessel disease, particularly in individuals with type 1 diabetes. Thus, we examined the relationship between psychomotor speed and resting state resting cerebral blood flow in a sample of adults with diabetes onset during childhood (≤ 17 years of age). The sample included 77 patients (39 M, 38 F) with a mean age of 47.43 ± 5.72 years, age of onset at 8.50 ± 4.26 years, and duration of disease of 38.92 ± 4.18 years. Resting cerebral blood flow was quantified using arterial spin labeling. After covarying for sex, years of education and normalized gray matter volume, slower psychomotor speed was associated with lower cerebral blood flow in bilateral caudate nucleus-thalamus and a region in the superior frontal gyrus. These results suggest that the basal ganglia and frontal cortex may underlie slower psychomotor speed in individuals with type 1 diabetes.

John P. Ryan, ryanjp@upmc.edu.

Author contributions JPR analyzed the data and wrote the manuscript; HJA oversaw data analysis and processing; TJO is responsible for recruitment and maintenance of the cohort; KAN oversaw data collection, management and assisted in manuscript preparation; HK performed data analyses and assisted in manuscript preparation; CR designed the study, oversaw data collection/management, and assisted in manuscript preparation.

Conflict of interest The authors have no conflicts of interest to disclose.

Compliance with ethical standards

All participants provided written informed consent prior to study participation. The University of Pittsburgh Institutional Review Board approved the study.

Electronic supplementary material The online version of this article (https://doi.org/10.1007/s11682–017-9783-y) contains supplementary material, which is available to authorized users.

Keywords

Arterial spin labeling; Cerebral blood flow; Cognition; Diabetes

Introduction

Individuals with type 1 diabetes mellitus (T1DM) are living longer and progressing into older age(Miller et al. 2012). In midlife, diabetes is associated with several neurocognitive complications, most notably impairments in psychomotor speed (PS), which is associated with greater risk of falls and poor self-care management (Feil et al. 2012; Wong et al. 2014). Although the phenomenon of slowed PS in T1DM is well documented, the potential neural mechanisms underlying this impairment are not yet understood. Slowed PS has been associated with later-stage vascular markers such as white matter hyperintensities (WMH), both in individuals with T1DM (Nunley et al. 2015) and in healthy aging populations (Jacobs et al. 2013).

Arterial spin labeling (ASL), is a noninvasive imaging method that uses magnetic labeling of protons in the blood to provide a measure of tissue cerebral blood flow (CBF) (Alsop et al. 2015; Detre et al. 2012; Detre and Wang 2002; Wolk and Detre 2012). Individuals with T1DM have lower gray matter CBF (Quirce et al. 1997) and blunted cerebral hemodynamic responses particularly among individuals with more severe hyperglycemia(Jiménez-Bonilla et al. 2001; Tagougui et al. 2015). Both chronic and acute hyperglycemia are associated with decreases in CBF, suggesting that more poorly controlled diabetes leads to alterations in CBF (Duckrow 1995; Kikano et al. 1989). Thus, ASL provides a unique advantage to examine differences in CBF that associate with cognitive changes that occur in conjunction with disease.

The basal ganglia are subcortical structures that regulate PS (Graybiel et al. 1994). Changes in CBF distribution in the basal ganglia have been linked to PS deficits in schizophrenia(Wright et al. 2015), and slower PS has been associated with hypoperfusion within the caudate nucleus in individuals with mild cognitive impairment and mild Alzheimer’s disease(Terada et al. 2013). Thus, basal ganglia CBF may provide insight into PS decrements that are commonly seen in individuals with T1DM. In non diabetic populations, the basal ganglia are especially vulnerable to SVD due to their poor collateral vascularization (watershed areas) (Pantoni 2010). The basal ganglia appear especially vulnerable to T1D, as shown by our group (Hughes et al. 2013; Hwang et al. 2016; Nunley et al. 2017) and others (Bolo et al. 2015a; Cranston et al. 2001; Gallardo-Moreno et al. 2015; Heikkilä et al. 2010; Moulton et al. 2015; Pell et al. 2012; Rooijackers et al. 2016; Seaquist 2015; Selvarajah et al. 2011). Abnormalities in the basal ganglia is of concern in T1D, because of their role in hypoglycemia unawareness(Bolo et al. 2015a; Cranston et al. 2001; Heikkilä et al. 2010; Rooijackers et al. 2016), as well as in decision making(Mogenson et al. 1980), thus potentially affecting diabetes management.

The goal of the present study was to identify associations between PS and resting state regional CBF in a cohort of middle-aged adults with childhood-onset T1DM. We

hypothesized that slower PS would be associated with lower CBF in the basal ganglia, as measured by using ASL.

Materials and methods

Participants were recruited from the Epidemiology of Diabetes Complications study at the University of Pittsburgh. The cohort comprises individuals with childhood onset (≤ 17 years of age) of T1DM who were seen within 1 year of their diagnosis at Children's Hospital of Pittsburgh (Pambianco et al. 2006; Wagener et al. 1982). Initial clinical assessments occurred in 1986–1988, including a 24-year follow-up that included 263 patients. Patients were invited to participate in an auxiliary study utilizing magnetic resonance imaging (MRI) and neuropsychology testing. MRI and neuropsychology data were collected on the same visit day. Of the 154 who volunteered to participate, 112 were eligible for MRI scanning and 101 had complete resting ASL data. Previous research on this cohort has identified a potential survivor bias for participants diagnosed before January 1, 1965 (Miller et al. 2012), and the 19 participants who met this criterion were excluded from analysis. An additional 5 participants were missing neuropsychology data, resulting in a final sample of 77 individuals. Of the 77 participants included in analyses, 66 (88%) self-reported as right-handed and 9 (11%) were left-handed. Participant characteristics are displayed in Table 1. Participants gave written informed consent and the University of Pittsburgh Institutional Review Board approved the study.

Neuropsychological battery

Psychomotor speed was measured using three cognitive tests: Digit Symbol Substitution Test (DSST, number correct in 90 s), Grooved Pegboard Task (GP, dominant hand, time to insert pegs, in seconds) and Trails Making Test, Part A (TMTA, seconds to complete). Cognitive test scores were normalized using SPSS v.22. Z-scores of the three tasks assessing psychomotor speed were summed then averaged to create a composite z-score. For the two tasks in which a higher score reflects poorer performance (i.e., GP and TMTA), signs were first reversed before calculating the average domain z-score. In addition to PS, the battery also tested other domains: Executive function (Stroop Color: Word Test; Verbal Fluency F-A-S; Letter-Number Sequence; Trail Making Test Part B[TMTB]; Ratio TMTB:TMTA); Memory (Rey Auditory Verbal Learning [Sum Trials 1–5, Interference, Delayed recall]; Four Word Short Term Memory 5-, 15-, and 30-second lists; Rey Osterrieth Complex Figure - Delayed Recall). Summary neuropsychology data for the present study are displayed in Supplementary Table S1. Neuropsychology data within the full cohort are published elsewhere (Nunley et al. 2015).

MRI data acquisition

All neuroimaging data were acquired on a 3T Trio TIM whole-body scanner (Siemens), with a 12-channel, phase-darray head coil. An axial, whole brain, T1-weighted three-dimensional magnetization-prepared rapid gradient echo (MPRAGE) anatomical image was collected (field of view (FOV) = 256 × 224 mm; repetition time (TR) = 2300 msec; inversion time (TI) = 900 msec; echo time (TE) = 3.43 msec; flip angle (FA) = 9 degrees, 176 slices; 1 mm

isotropic resolution, no gap). To estimate white matter hyperintensities (WMH), we collected an axial, whole brain fluid-attenuated inversion recovery image, or FLAIR, (FOV = 212 × 256 mm; TR = 9160 ms; TI = 2500 ms; TE = 90 ms; FA = 150; 48 slices; 1 × 1 × 3 mm resolution).

Resting CBF was acquired with a pulsed ASL sequence. Participants were instructed to view a white cross hair and remain awake. For this sequence, interleaved labeled and unlabeled images were obtained over a 5-minute, 28-second period using gradient-echo echo-planar imaging. The pulsed ASL sequence used a modified flow-sensitive alternating inversion recovery method, applying a saturation pulse 700 ms after an inversion pulse. To reduce transit artifact, a 1000-ms delay separated the end of the labeling pulse and the time of image acquisition. Resting ASL image acquisition parameters were: FOV = 240 × 240 mm; TR = 4000 ms; TE = 18 ms; and FA = 90°. Twenty-two slices (4 mm thick, 1 mm gap) were acquired sequentially in an inferior-to-superior direction for each brain image, yielding 80 total images (40 labeled and 40 unlabeled; with 3 initial discarded images allowing for magnetic equilibration). Two additional unlabeled (control) images using the same parameters but a longer TR (8000 ms) were acquired as reference for the equilibrium brain tissue magnetization.

Image processing

Preprocessing was performed in SPM8 (Wellcome Trust Centre for Neuroimaging; http://www.fil.ion.ucl.ac.uk/ spm/software/spm8/). Resting ASL images were motion corrected (labeled and unlabeled images were separately corrected and then jointly corrected) to the first image of the series by rigid body transformation (mutual information similarity metric and 4th degree B-spline interpolation), then smoothed with a 10 mm full-width at half-maximum isotropic Gaussian kernel. Similar processing was done on the equilibrium magnetization images. CBF calculation was performed using a script in MatLab by Wang et al.(Wang et al. 2003) The following parameters were utilized in the script: surround subtraction method, label time of 0.7, delay time of 1.2, slice time of 45, labeling efficiency of 0.95, and TE of 18 ms. The equilibrium magnetization image was used to further improve the CBF estimate. CBF estimates were only calculated in the image if they passed a height threshold of 500 MR units (relative). CBF maps were normalized (coregistered) into MNI space. Each participant's MPRAGE was segmented into gray matter, white matter, and cerebrospinal fluid. We then coregistered the gray matter image to the mean ASL image (via an affine coregistration with normalized mutual information similarity metric and no interpolation – only the transformation matrix was stored). This coregistered structural gray matter segmentation was then coregistered to a template gray matter segmentation (nonlinear warping) with a final resolution of 4 mm isotropic resolution (Supplementary Figure S1). We then used FSL (fslmaths) to calculate the mean CBF image.

An Automated Labeling Pathway was used to calculate whole brain and regional counts of gray matter, white matter, and cerebrospinal fluid in the MPRAGE (Wu et al. 2006). Briefly, this method uses FMRIB Software Library's () Brain Extraction Tool to first extract a mask of the intracranial volume. Trained lab members further corrected these maps using ITK-SNAP (http://www.itksnap.org/). This was used to calculate the intracranial volume. Next,

FSL's FLIRT was utilized to perform a linear (affine) coregistration between the MPRAGE and the templates. Then ITK-Toolkit (https://itk.org/) was used to perform a fully deformable coregistration. Importantly, all processing was done from the template space to the native space, which allows for greater flexibility within subject. This process results in segmentations of the gray, white, and CSF that can be used to calculate volumes for each class. Normalized gray matter volume index was calculated by dividing whole brain gray matter volume by intracranial volume (O'Brien et al. 2011). To calculate WMH burden, we utilized a previously established automated segmentation algorithm that involves automatic seed selection and fuzzy connectedness (Wu et al. 2006). All segmentations of WMH were visualized by human eye for quality. Normalized global burden was the amount of WMH voxels divided by intracranial volume. Five participants were missing WMH data and were excluded from the supplementary correlation analysis.

To limit regions of analysis to gray matter, we created a study specific gray matter mask. We also created a normalized structural image that was the average across subjects. This stage of the processing was completed in SPM12. We segmented each MPRAGE into six tissue classes (gray matter, white matter, cerebrospinal fluid, soft-tissue, skull, and air). We then generated an automatic intracranial volume mask for each subject (threshold GM, WM, CSF with probability greater than 0.1 then an image filling and image closing algorithm [sphere of one voxel]). We applied that mask to the MPRAGE. We normalized the skull-stripped MPRAGE into MNI space (same resolution as the ASL maps)—this image was used to overlay the CBF imaging results. Normalized segmentations (probability maps) were used to determine a label for each voxel which converted tissue type maps into binary images. Tissue type was determined by assigning a voxel to a tissue type if it has the maximum probability between tissue types. We generated a tissue probability map by adding all binary segmentations across subjects then dividing by the number of subjects to generate a study specific probability map. We then determined the study specific gray matter mask by assigning voxels to a tissue type if it has the maximum probability among tissue types. This mask was down-sampled to the same resolution as the ASL maps using nearest-neighbor interpolation.

Statistical methods

Gray matter analyses were performed using the statistical nonparametric mapping (SnPM) toolbox (http://warwick.ac.uk/snpm). Subject CBF maps were entered into separate group-level regressions with PS as the predictor of interest. Age, degree of normalized gray matter volume, years of education, and sex were included as nuisance covariates. These were included as they significantly associated with CBF. Other variables that were investigated but not included were memory and executive function domain z-scores and WMH burden. Data were analyzed using permutation testing with cluster-level inference (5000 permutations, cluster forming threshold $p = 0.001$, FWE corrected $p < 0.05$) with the study specific gray matter mask. SPSS (v.22, IBM) was used for correlation analyses examining the relationship between cluster CBF and other neuropsychological and clinical variables using bivariate correlations. Due to the missing WMH data from 5 participants, *post hoc* partial correlation analyses were performed to examine the relationship between PS and CBF independent of WMH burden.

Results

Participant characteristics are displayed in Table 1. The sample included 77 patients (39 M, 38 F) with a mean age of 47.43(± 5.72) years, age of onset at 8.50 (± 4.26) years, and duration of disease of 38.92 (± 4.18) years.

Slower PS was associated with lower CBF in a cluster encompassing the bilateral caudate nucleus and thalamus (Fig. 1; peak t = 4.24; p value at peak-t = 3.1×10^{-5}; x, y, z = − 2, − 4, 2; $k_{voxels} = 48$), as well as a separate cluster in the frontal lobe including bilateral superior frontal gyrus (Fig. 1; peak t = 4.79; p value at peak-t = 3.9×10^{-6}; x, y, z = − 14, 52, 38; $k_{voxels} = 55$). There were no regions in which faster PS was associated with lower CBF. Scatterplots of the relationship between PS and extracted cluster CBF are displayed in Fig. 2. Summary data of CBF and WMH are shown in Table 2.

To examine the specificity of the clusters for PS, separate whole brain voxel-wise models were run with z-scores for memory and executive functioning as independent predictors of CBF. There were no regions of CBF that associated with memory or executive functioning domain z-scores. Moreover, log-transformed WMH volumes were associated with slower PS ($r(72) = -0.29$, $p = 0.01$) but WMH burden did not associate with either CBF cluster ($p > 0.18$). Adjusting for WMH volume did not eliminate the association between PS and CBF (caudate: $r(69) = 0.37$, $p = 0.001$; superior frontal: $r(69) = 0.37$, $p = 0.002$). Associations between extracted cluster values and clinical variables are displayed in Table 3. PS was associated with age and duration of disease, and CBF in the superior frontal cluster was associated with body mass index.

Discussion

In this group of middle-aged individuals with childhood onset T1DM, slower PS was associated with lower CBF in the basal ganglia and superior frontal gyrus. CBF values were not associated with memory or executive functioning domains suggesting that the association was specific to PS. CBF values were not associated with WMH, and adjusting for WMH did not eliminate the relationship between PS and CBF. These findings suggest that in middle-aged adults with childhood onset T1DM, differences in PS are associated with CBF and this association is specific to the basal ganglia and superior frontal gyrus and not influenced by other measures of lower brain integrity.

Previous longitudinal research has identified micro- and macro-vascular complications of T1DM as predictors of decline in PS(Ryan et al. 2003). Although CBF was not related to whole brain WMH volume, previous research has demonstrated that reductions in CBF may precede development of leukoariosis (Bernbaum et al. 2015) and could potentially be a preclinical biomarker for the development of neurological dysfunction(Hays et al. 2016). Longitudinal studies will be required to understand the implications of individual differences in CBF, and if over time these effects remain limited to PS, or if they will become more diffuse and begin to associate with other neuropsychological domains.

The localization of the findings to regions of the basal ganglia, particularly the caudate nucleus and thalamus, are noteworthy given the centrality of the basal ganglia in movement

and cognition. Striatal areas have previously been associated with cognitive slowing in Parkinson's disease(Jokinen et al. 2013), and caudate volume predicts PS in older depressed individuals(Naismith et al. 2002), as well as individuals with multiple sclerosis(Batista et al. 2012). The finding that slower PS is linked to lower CBF within the basal ganglia contributes to previous findings highlighting the vulnerability of subcortical regions in individuals with T1DM. The functional connectivity of the basal ganglia is altered in response to hypoglycemia in individuals with T1DM (Bolo et al. 2015b), and changes in basal ganglia volume have been documented in a pediatric sample of individuals with T1DM(Northam et al. 2009). These data build upon findings in the basal ganglia by our group (Hughes et al. 2013; Hwang et al. 2016; Nunley et al. 2017) and others (Bolo et al. 2015a; Cranston et al. 2001; Gallardo-Moreno et al. 2015; Heikkilä et al. 2010; Moulton et al. 2015; Pell et al. 2012; Rooijackers et al. 2016; Seaquist 2015; Selvarajah et al. 2011).

There are several limitations of the present study that should be noted. First, the ASL data were collected during rest rather than during a PS task. Further research on ASL and BOLD reactivity during task performance may increase our understanding of the neural dynamics during task performance. Second, the cross-sectional nature of the present dataset precludes inferences of causality. Future longitudinal studies of this cohort will enable us to identify any potential progression of changes in cognition, and understand if individual differences in CBF are a biomarker of future cognitive decline, or development of other vascular pathology. Our study is only able to show that lower CBF is cross-sectionally associated with lower PS, and with no healthy control group it cannot be determined how these results relate to such a sample. Previous studies have found that CBF is not different between adults with T1DM and controls(van Golen et al. 2013), thus it is unclear if our findings are specific to individuals with T1DM. Strengths of the present study include the relatively large number of participants in a well-characterized cohort of individuals with T1DM, as well as the broad neuropsychological battery that was administered. Additionally, by utilizing three measures of PS that draw upon fine motor control (pegboard) and tasks that draw upon higher levels of cognition (DSST), we have sampled a relatively broad domain of PS.

In summary, slower PS is a common problem in individuals with T1DM. The neural underpinnings of this association are not clear. We identified differences in regional cerebral CBF–particularly in the basal ganglia–that associate with slower PS. Further longitudinal research will be needed to understand the clinical and long-term implications of individual differences in CBF.

Supplementary Material

Refer to Web version on PubMed Central for supplementary material.

Acknowledgements

The authors wish to acknowledge Dr. Christopher Ryan and Dr. Judith Saxton for their assistance in the development and administration of the neuropsychology protocol.

Funding This study was funded by National Institutes of Health grants DK095759 (Ryan), AG037451 (Rosano), DK089028 (Rosano), AG024827 (Rosano), DK034818 (Orchard) and the Rossi Memorial Fund (Orchard).

Sources of support DK095759 (Ryan), AG037451 (Rosano), DK089028 (Rosano), AG024827 (Rosano), DK034818 (Orchard), and the Rossi Memorial Fund (Orchard).

References

Alsop DC, Detre JA, Golay X, Günther M, Hendrikse J, Hernandez-Garcia L, … Zaharchuk G (2015). Recommended implementation of arterial spin-labeled perfusion MRI for clinical applications: a consensus of the ISMRM perfusion study group and the European consortium for ASL in dementia. Magnetic Resonance in Medicine, 73(1), spcone. 10.1002/mrm.25607.

Batista S, Zivadinov R, Hoogs M, Bergsland N, Heininen-Brown M, Dwyer MG, … Benedict RHB (2012). Basal ganglia, thalamus and neocortical atrophy predicting slowed cognitive processing in multiple sclerosis. Journal of Neurology, 259(1), 139–146. 10.1007/s00415-011-6147-1. [PubMed: 21720932]

Bernbaum M, Menon BK, Fick G, Smith EE, Goyal M, Frayne R, & Coutts SB (2015). Reduced blood flow in normal white matter predicts development of leukoaraiosis. Journal of Cerebral Blood Flow and Metabolism: Official Journal of the International Society of Cerebral Blood Flow and Metabolism, 35(10), 1610–1615. 10.1038/jcbfm.2015.92.

Bolo NR, Musen G, Simonson DC, Nickerson LD, Flores VL, Siracusa T, … Jacobson (2015a). Functional connectivity of insula, basal ganglia, and prefrontal executive control networks during hypoglycemia in type 1 diabetes. The Journal of Neuroscience: The Official Journal of the Society for Neuroscience, 35(31), 11012–11023. 10.1523/JNEUROSCI.0319-15.2015. [PubMed: 26245963]

Bolo NR, Musen G, Simonson DC, Nickerson LD, Flores VL, Siracusa T, … Jacobson AM (2015b). Functional connectivity of insula, basal ganglia, and prefrontal executive control networks during hypoglycemia in type 1 diabetes. The Journal of Neuroscience: The Official Journal of the Society for Neuroscience, 35(31), 11012–11023. 10.1523/JNEUROSCI.0319-15.2015. [PubMed: 26245963]

Cranston I, Reed LJ, Marsden PK, & Amiel SA (2001). Changes in regional brain (18)F-fluorodeoxyglucose uptake at hypoglycemia in type 1 diabetic men associated with hypoglycemia unawareness and counter-regulatory failure. Diabetes, 50(10), 2329–2336. [PubMed: 11574416]

Detre JA, Rao H, Wang DJJ, Chen YF, & Wang Z (2012). Applications of arterial spin labeled MRI in the brain. Journal of Magnetic Resonance Imaging: JMRI, 35(5), 1026–1037. 10.1002/jmri.23581. [PubMed: 22246782]

Detre JA, & Wang J (2002). Technical aspects and utility of fMRI using BOLD and ASL. Clinical Neurophysiology, 113, 621–634. 10.1016/S1388-2457(02)00038-X. [PubMed: 11976042]

Duckrow RB (1995). Decreased cerebral blood flow during acute hyperglycemia. Brain Research, 703(1–2), 145–150. [PubMed: 8719626]

Feil DG, Zhu CW, & Sultzer DL (2012). The relationship between cognitive impairment and diabetes self-management in a population-based community sample of older adults with Type 2 diabetes. Journal of Behavioral Medicine, 35(2), 190–199. 10.1007/s10865-011-9344-6. [PubMed: 21503710]

Gallardo-Moreno GB, González-Garrido AA, Gudayol-Ferré E, & Guàrdia-Olmos J (2015). Type 1 diabetes modifies brain activation in young patients while performing visuospatial working memory tasks. Journal of Diabetes Research, 2015, 703512 10.1155/2015/703512. [PubMed: 26266268]

Graybiel AM, Aosaki T, Flaherty AW, & Kimura M (1994). The basal ganglia and adaptive motor control. Science (New York), 265(5180), pp. 1826–1831.

Hays CC, Zlatar ZZ, & Wierenga CE (2016). The utility of cerebral blood flow as a biomarker of preclinical Alzheimer's disease. Cellular and Molecular Neurobiology. 10.1007/s10571-015-0261-z.

Heikkilä O, Lundbom N, Timonen M, Groop P-H, Heikkinen S, & Mäkimattila S (2010). Evidence for abnormal glucose uptake or metabolism in thalamus during acute hyperglycaemia in type 1 diabetes—a 1H MRS study. Metabolic Brain Disease, 25(2), 227–234. 10.1007/s11011-010-9199-5. [PubMed: 20424902]

Hughes TM, Ryan CM, Aizenstein HJ, Nunley K, Gianaros PJ, Miller R, … Rosano C (2013). Frontal gray matter atrophy in middle aged adults with type 1 diabetes is independent of cardiovascular risk factors and diabetes complications. Journal of Diabetes and Its Complications, 27(6), 558–564. 10.1016/j.jdiacomp.2013.07.001. [PubMed: 23994432]

Hwang M, Tudorascu DL, Nunley K, Karim H, Aizenstein HJ, Orchard TJ, & Rosano C (2016). Brain activation and psychomotor speed in middle-aged patients with type 1 diabetes: relationships with hyperglycemia and brain small vessel disease. Journal of Diabetes Research, 2016, 9571464 10.1155/2016/9571464. [PubMed: 26998494]

Jacobs HIL, Leritz EC, Williams VJ, Van Boxtel MPJ, van der Elst W, Jolles J, … Salat DH (2013). Association between white matter microstructure, executive functions, and processing speed in older adults: the impact of vascular health. Human Brain Mapping, 34(1), 77–95. 10.1002/hbm.21412. [PubMed: 21954054]

Jiménez-Bonilla JF, Quirce R, Hernández A, Vallina NK, Guede C, Banzo I, … Carril JM (2001). Assessment of cerebral perfusion and cerebrovascular reserve in insulin-dependent diabetic patients without central neurological symptoms by means of 99mTc-HMPAO SPET with acetazolamide. European Journal of Nuclear Medicine, 28(11), 1647–1655. 10.1007/s002590100595. [PubMed: 11702106]

Jokinen P, Karrasch M, Brück A, Johansson J, Bergman J, & Rinne JO (2013). Cognitive slowing in Parkinson's disease is related to frontostriatal dopaminergic dysfunction. Journal of the Neurological Sciences, 329(1–2), 23–28. 10.1016/j.jns.2013.03.006. [PubMed: 23561982]

Kikano GE, LaManna JC, & Harik SI (1989). Brain perfusion in acute and chronic hyperglycemia in rats. Stroke; a Journal of Cerebral Circulation, 20(8), 1027–1031.

Miller RG, Secrest AM, Sharma RK, Songer TJ, & Orchard TJ (2012). Improvements in the life expectancy of type 1 diabetes: the Pittsburgh Epidemiology of Diabetes Complications study cohort. Diabetes, 61(11), 2987–2992. 10.2337/db11-1625. [PubMed: 22851572]

Mogenson GJ, Jones DL, & Yim CY (1980). From motivation to action: functional interface between the limbic system and the motor system. Progress in Neurobiology, 14(2–3), 69–97. [PubMed: 6999537]

Moulton CD, Costafreda SG, Horton P, Ismail K, & Fu CHY (2015). Meta-analyses of structural regional cerebral effects in type 1 and type 2 diabetes. Brain Imaging and Behavior, 9(4), 651–662. 10.1007/s11682-014-9348-2. [PubMed: 25563229]

Naismith S, Hickie I, Ward PB, Turner K, Scott E, Little C, … Parker G (2002). Caudate nucleus volumes and genetic determinants of homocysteine metabolism in the prediction of psychomotor speed in older persons with depression. The American Journal of Psychiatry, 159(12), 2096–2098. 10.1176/appi.ajp.159.12.2096. [PubMed: 12450963]

Northam EA, Rankins D, Lin A, Wellard RM, Pell GS, Finch SJ, … Cameron FJ (2009). Central nervous system function in youth with type 1 diabetes 12 years after disease onset. Diabetes Care, 32(3), 445–450. 10.2337/dc08-1657. [PubMed: 19151204]

Nunley KA, Rosano C, Ryan CM, Jennings JR, Aizenstein HJ, Zgibor JC, … Saxton JA (2015). Clinically relevant cognitive impairment in middle-aged adults with childhood-onset type 1 diabetes. Diabetes Care, 38(9), 1768–1776. 10.2337/dc15-0041. [PubMed: 26153270]

Nunley KA, Ryan CM, Aizenstein HJ, MacCloud RL, Orchard TJ, & Rosano C (2017). Regional gray matter volumes as related to psychomotor slowing in adults with type 1 diabetes. Psychosomatic Medicine. 10.1097/PSY.0000000000000449.

Nunley KA, Ryan CM, Orchard TJ, Aizenstein HJ, Jennings JR, Ryan J, … Rosano C (2015). White matter hyperintensities in middle-aged adults with childhood-onset type 1 diabetes. Neurology, 84(20), 2062–2069. 10.1212/WNL.0000000000001582. [PubMed: 25904692]

O'Brien LM, Ziegler DA, Deutsch CK, Frazier JA, Herbert MR, & Locascio JJ (2011). Statistical adjustments for brain size in volumetric neuroimaging studies: some practical implications in methods. Psychiatry Research, 193(2), 113–122. 10.1016/j.pscychresns.2011.01.007. [PubMed: 21684724]

Pambianco G, Costacou T, Ellis D, Becker DJ, Klein R, & Orchard TJ (2006). The 30-year natural history of type 1 diabetes complications. Diabetes, 55(5), 1463–1469. 10.2337/db05-1423. [PubMed: 16644706]

Pantoni L (2010). Cerebral small vessel disease: from pathogenesis and clinical characteristics to therapeutic challenges. The Lancet Neurology, 9(7), 689–701. 10.1016/S1474-4422(10)70104-6. [PubMed: 20610345]

Pell GS, Lin A, Wellard RM, Werther GA, Cameron FJ, Finch SJ, … Northam EA (2012). Age-related loss of brain volume and T2 relaxation time in youth with type 1 diabetes. Diabetes Care, 35(3), 513–519. 10.2337/dc11-1290. [PubMed: 22301124]

Quirce R, Carril JM, Jiménez-Bonilla JF, Amado JA, Gutiérrez-Mendiguchía C, Banzo I, … Montero A (1997). Semi-quantitative assessment of cerebral blood flow with 99mTc-HMPAO SPET in type I diabetic patients with no clinical history of cerebrovascular disease. European Journal of Nuclear Medicine, 24(12), 1507–1513. [PubMed: 9391186]

Rooijackers HMM, Wiegers EC, Tack CJ, van der Graaf M, & de Galan BE (2016). Brain glucose metabolism during hypoglycemia in type 1 diabetes: insights from functional and metabolic neuroimaging studies. Cellular and Molecular Life Sciences: CMLS, 73(4), 705–722. 10.1007/s00018-015-2079-8. [PubMed: 26521082]

Ryan CM, Geckle MO, & Orchard TJ (2003). Cognitive efficiency declines over time in adults with Type 1 diabetes: effects of micro- and macrovascular complications. Diabetologia, 46(7), 940–948. 10.1007/s00125-003-1128-2. [PubMed: 12819900]

Seaquist ER (2015). The impact of diabetes on cerebral structure and function. Psychosomatic Medicine, 77(6), 616–621. 10.1097/PSY.0000000000000207. [PubMed: 26163815]

Selvarajah D, Wilkinson ID, Gandhi R, Griffiths PD, & Tesfaye S (2011). Microvascular perfusion abnormalities of the Thalamus in painful but not painless diabetic polyneuropathy: a clue to the pathogenesis of pain in type 1 diabetes. Diabetes Care, 34(3), 718–720. 10.2337/dc10-1550. [PubMed: 21282344]

Tagougui S, Fontaine P, Leclair E, Aucouturier J, Matran R, Oussaidene K, … Heyman E (2015). Regional cerebral hemodynamic response to incremental exercise is blunted in poorly controlled patients with uncomplicated type 1 diabetes. Diabetes Care, 38(5), 858–867. 10.2337/dc14-1792. [PubMed: 25665816]

Terada S, Sato S, Nagao S, Ikeda C, Shindo A, Hayashi S, … Uchitomi Y (2013). Trail making test B and brain perfusion imaging in mild cognitive impairment and mild Alzheimer's disease. Psychiatry Research, 213(3), 249–255. 10.1016/j.pscychresns.2013.03.006. [PubMed: 23830931]

van Golen LW, Kuijer JPA, Huisman MC, Ijzerman RG, Barkhof F, Diamant M, & Lammertsma AA (2013). Quantification of cerebral blood flow in healthy volunteers and type 1 diabetic patients: Comparison of MRI arterial spin labeling and [(15) O]H2 O positron emission tomography (PET). Journal of Magnetic Resonance Imaging: JMRI. 10.1002/jmri.24484.

Wagener DK, Sacks JM, LaPorte RE, & MaCgregor JM (1982). The Pittsburgh study of insulin-dependent diabetes mellitus: risk for diabetes among relatives of IDDM. Diabetes, 31(2), 136–144. 10.2337/diab.31.2.136. [PubMed: 6759229]

Wang J, Aguirre GK, Kimberg DY, Roc AC, Li L, & Detre JA (2003). Arterial spin labeling perfusion fMRI with very low task frequency. Magnetic Resonance in Medicine: Official Journal of the Society of Magnetic Resonance in Medicine / Society of Magnetic Resonance in Medicine, 49(5), 796–802. 10.1002/mrm.10437.

Wolk DA, & Detre JA (2012). Arterial spin labeling MRI: an emerging biomarker for Alzheimer's disease and other neuro-degenerative conditions. Current Opinion in Neurology, 25(4), 421–428. 10.1097/WCO.0b013e328354ff0a. [PubMed: 22610458]

Wong RHX, Scholey A, & Howe PRC (2014). Assessing premorbid cognitive ability in adults with type 2 diabetes mellitus–a review with implications for future intervention studies. Current Diabetes Reports, 14(11), 547 10.1007/s11892-014-0547-4. [PubMed: 25273482]

Wright SN, Hong LE, Winkler AM, Chiappelli J, Nugent K, Muellerklein F, … Kochunov P (2015). Perfusion shift from white to gray matter may account for processing speed deficits in schizophrenia. Human Brain Mapping, 36(10), 3793–3804. 10.1002/hbm.22878. [PubMed: 26108347]

Wu M, Rosano C, Butters M, Whyte E, Nable M, Crooks R, … Aizenstein HJ (2006). A fully automated method for quantifying and localizing white matter hyperintensities on MR images. Psychiatry Research, 148(2–3), 133–142. 10.1016/j.pscychresns.2006.09.003. [PubMed: 17097277]

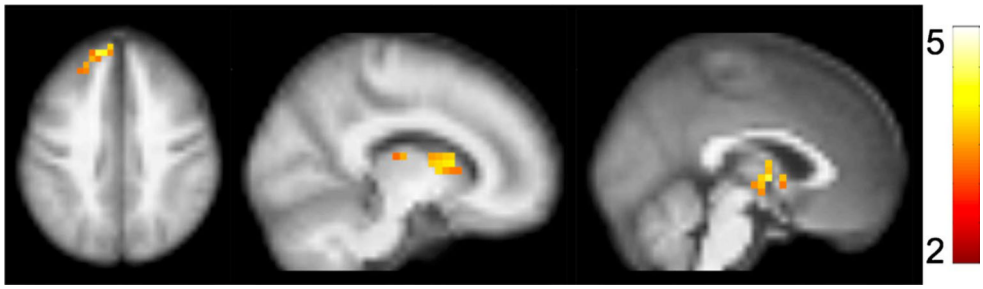

Fig. 1.

Associations between processing speed (PS) and cerebral blood flow (CBF). Slower PS was associated with lower CBF in two clusters: one encompassing bilateral caudate nucleus and thalamus (peak t = 4.24; p value at peak-t = 3.1×10^{-5}; x, y, z = − 2, − 4, 2; k_{voxels} = 48), as well as a separate cluster in the frontal lobe including bilateral superior frontal gyrus (Fig. 1; peak t = 4.79; p value at peak- t = 3.9×10^{-6}; x, y, z = − 14, 52, 38; k_{voxels} = 55). Activation clusters are overlaid on a 4 mm resolution brain image generated by averaging across all subject-specific structural images

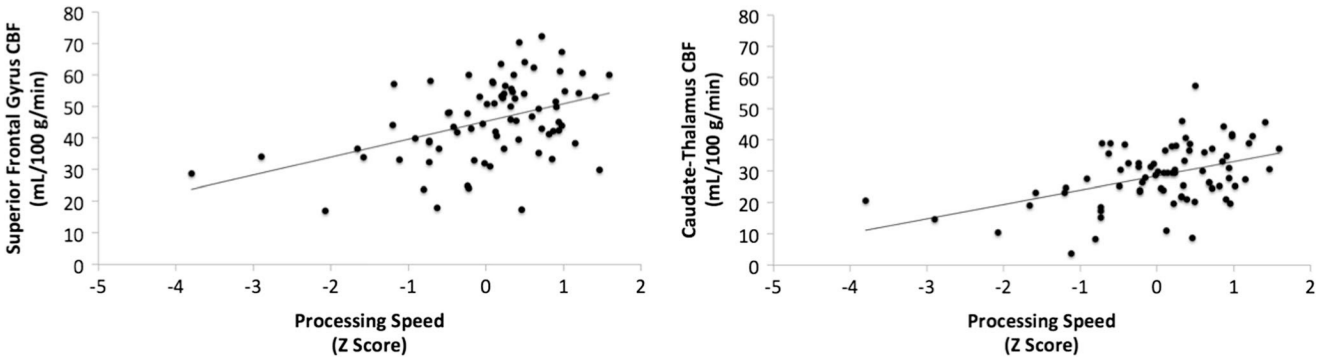

Fig. 2.

Scatterplots displaying associations between PS (domain z-scores) and CBF (mL/100 g/min) in each cluster

Table 1

Sample characteristics

Variable	M ± SD (Range)
Age (years)	47.43 ± 5.72 (32.2–58.5)
Sex	39 M / 38 F
Years of education	14.97 ± 2.41 (10–21)
Disease duration (years)	38.92 ± 4.18 (31.5–46.5)
HbA1c (%)	7.80 ± 1.41 (5.3–14.1)
Body mass index (kg/m^2)	27.49 ± 4.69 (18.6–38.9)
Systolic blood pressure (mmHg)	118.16 ± 15.25 (86–154)
Diastolic blood pressure (mmHg)	66.00 ± 9.09 (40–86)

Table 2

Summary of cerebral blood flow values for gray and white matter, and the two clusters of significance

Variable	M ± SD
Gray matter CBF (mL/100 g/min)	45.79 ± 7.84
White matter CBF (mL/100 g/min)	49.29 ± 8.38
Caudate-Thalamus CBF (mL/100 g/min)	32.70 ± 8.73
Superior frontal CBF (mL/100 g/min)	46.52 ± 12.24
White matter hyperintensity	.003 ± .0004
Gray matter atrophy	33.74 ± 2.18

Raw white matter hyperintensity values are displayed, but were log-transformed prior to analyses due to skew

Table 3

Bivariate Pearson's correlations between clinical variables, psychomotor speed (PS) and CBF in caudate-thalamus and superior frontal clusters

Variable	Age	Duration	a1cmon	BMI	A1cMRI	SBP	DBP	nGMV
Caudate-Thalamus	− 0.20	− 0.11	− 0.06	− 0.14	− 0.07	− 0.01	− 0.02	0.19
Superior Frontal	− 0.12	− 0.07	− 0.55	− 0.28*	− 0.06	− 0.21	− 0.11	0.09
PS	− 0.31**	− 0.25*	− 0.07	− 0.14	− 0.08	− 0.11	0.01	0.16

a1cmon, a1c months at MRI; *BMI*, body mass index; *A1c*, A1c measured at MRI scan; *SBP*, systolic blood pressure; *DBP*, diastolic blood pressure; *nGMV*, Normalized gray matter volume (ratio of gray matter volume to intracranial volume)

* $p < 0.05$,

** $p < 0.01$